

## Results of Outgoing Longwave Radiation and Albedo over Saudi Arabia from Earth Radiation Budget Experiment (ERBE) Data

A.K. AL-KHALAF

*Dept. of Meteorology, Faculty of Meteorology, Environment, and Arid Land Agriculture King Abdulaziz University, Jeddah, Kingdom of Saudi Arabia*

ABSTRACT. Changes in the albedo and outgoing longwave radiation at the top of the atmosphere derived from Earth Radiation Budget Experiment (ERBE) are specified as a function of atmospheric (all sky conditions) and surface properties (clear sky conditions). Albedo and outgoing longwave radiation observations are also used to relate cloudiness variations to regional features of the general circulations such as precipitation zones, persistent cloudiness, and areas of subsidence. A method requiring only measurements of outgoing long wave radiation and planetary albedo is applied to evaluate the relative importance of the albedo and long wave radiation on the atmospheric circulation. The approach of studying these observations in time and space is also used to examine the radiative energy budget of different geographic locations such as deserts, high land, and coastal areas. The results indicate that there are clear relationships between the variability in outgoing longwave radiation, albedo, and features of the atmospheric circulation, which appear to be linked to changes in cloudiness. In addition, the effect of geographical variations of Saudi Arabia on cloud is analyzed and related to circulation features. The longwave mean ranges from  $257.1 \text{ Wm}^{-2}$  to  $307.7 \text{ Wm}^{-2}$ , and the longwave standard deviation ranges from  $10.6 \text{ Wm}^{-2}$  to  $27.9 \text{ Wm}^{-2}$  over the region. The albedo mean ranges from 20.9% to 30.6%, and the albedo standard deviation ranges from 5.5% to 8.7% over the region. The longwave cloud forcing at the top of the atmosphere equals  $15 \text{ Wm}^{-2}$  for January,  $22 \text{ Wm}^{-2}$  for April,  $14 \text{ Wm}^{-2}$  for July, and  $10 \text{ Wm}^{-2}$  for October 1989. Thus compared to a cloud free atmosphere, the January mean cloudiness, as it was present, reduces the outgoing longwave radiation for the total earth-atmosphere system by about 6%, for the month of April by about 8%, for the month

of July by about 5%, and for the month of October by about 3%. For clear sky desert conditions, a weak relationship ( $R^2 = 0.38$ ) between the albedo and outgoing longwave radiation was found at some locations over the Kingdom. Whereas the relationship between all sky albedo and all sky outgoing longwave radiation results in a strong relationship ( $R^2 = 0.80$ ) at some locations.

## 1. Introduction

The global energy balance is important for Earth's climate. When visible radiation from the Sun reaches the Earth and the sky is clear, some is reflected or scattered directly back into space as shortwave radiation (the percent reflected is known as albedo), and some is absorbed by the Earth. When the radiation is absorbed by the Earth's surface, it re-emits this energy at a longer wavelength. When clouds are present, the radiation balance becomes more complicated than in clear sky cases. The radiation balance of the earth as observed by earth-orbiting satellites has been of concern to atmospheric scientists since the mid-1960s. In 1975 a major advance in measuring the earth radiation budget was made with the earth radiation budget (ERB) experiment (Smith *et al.*, 1977). The ERB instruments made broadband observations that were significant for climate studies. Most of these satellites move in polar, sun-synchronous orbits that allow twice daily global observations of weather patterns.

The ERB data from past satellites have improved our understanding of the global climate system of the earth (Jacobowitz *et al.*, 1979) and recent ERB measurements systems added much more to our understanding of global, regional and local diurnal heat budgets. The largest day-to-day variations in the earth planetary albedo and outgoing thermal radiation are caused by variation in clouds. Satellite borne instruments have been developed and deployed to measure the (ERB) at the top of the atmosphere (Bess and Smith, 1993). Clouds play an important role in determining the present climate and climate sensitivity that leads to a change of climatic parameters (Manabe and Wetherald, 1967). Since clouds have much strong influence in ERB measurements, and the radiation at the top of the atmosphere is so central in the maintenance of climate, a relationship between clouds and climate can be found by studying ERB data.

Clouds have two important effects on the radiation budget of the earth-atmosphere system. As a result of their scattering properties at solar radiation wavelengths, they act to increase the albedo of the system, and an increased albedo means a reduction in the amount of absorbed solar radiation. As a result of their absorption properties at terrestrial radiation wavelengths, they act to increase the longwave radiation loss to space. To fully understand the coupling between climate and perturbations in the (ERB), research must address the

physical relationship between changing atmospheric and surface conditions and resultant changes in the ERB (Ackerman and Inoue, 1994).

In this paper, ERB observations investigate the sensitivity of fluxes at the top of the atmosphere in changing atmospheric and surface properties. Longwave flux, cloud forcing, and albedo for the Saudi Arabia are analyzed from the monthly ERB data for 1989. ERB data can enhance our knowledge of how clouds and albedo affect the radiation distribution and the atmospheric general circulation of the atmosphere.

## 2. Data Description

The Earth Radiation Budget Experiment (ERBE) was designed to collect information about sunlight reaching the Earth, sunlight reflected by the Earth, and heat released by the Earth into space. Since October 1984, ERBE employed three satellites to carry the instruments which collected this information: ERBS, NOAA-9, and NOAA-10. Each satellite was equipped with special instruments (scanners) that measured radiation along the satellite track and from space. Radiation was measured in three wavelength bands: total radiation in the 0.2 to 50 micron wavelength band, longwave radiation in the 5 to 50 micron wavelength band, and shortwave radiation in the 0.2 to 5 micron wavelength band (Barkstrom *et al.*, 1989).

As indicated above, the ERB data include shortwave (solar) radiation reflected by the Earth's surface and longwave radiation emitted by the Earth. Albedo is computed as the ratio between the shortwave radiation reflected from Earth and the shortwave radiation coming in from space. Clear sky albedo is the light reflected back only from cloudless areas of Earth's surface whereas all sky albedo is the light reflected back only from cloudy areas of the Earth's surface. These data are processed by month for the duration of the satellite flight, and are provided on a grid of latitude and longitude lines. On this grid, longitude varies from 1.25°E to 1.25°W by intervals of 2.5° (*i.e.* longitude varies from 1.25°E to 358.75°E), and latitude varies from 88.75°N to 88.75°S by intervals of 2.5°. Thus there are 144 grid points on each latitude and 72 latitudes overall. The selected study area of Saudi Arabia ranges from 15°N to 30°N latitude and from 35°E to 55°E longitude.

## 3. Geographical Distributions of Longwave and Albedo

The result of absorption of solar radiation at Earth's surface is heating Earth which radiates it back to space. Since Earth is cool relative to sun, its radiation to space peaks in the infrared (long wavelength) band of the electromagnetic spectrum. Because some components of Earth's atmosphere trap longwave ra-

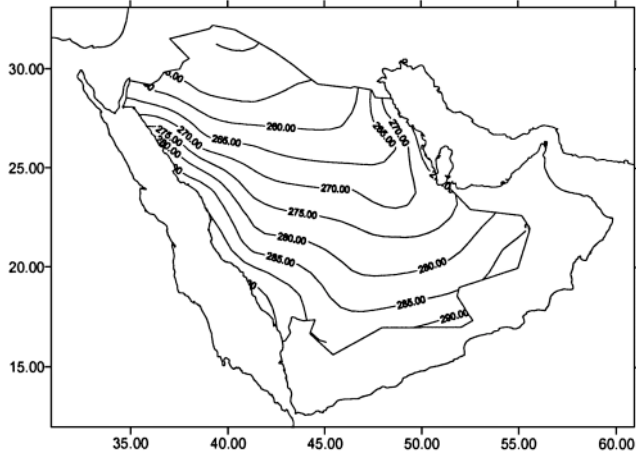
diation (the greenhouse effect), emission to space occurs not at Earth's surface, but at a level in the atmosphere which depends on the concentration of greenhouse gases at that location. Therefore, geographic variations in these data set are a result of differences in the effective temperature (the temperature at which the planet is emitting to space) at various locations. Effective temperature depends both on the temperature at the surface, and on the concentrations and vertical profiles of greenhouse gases.

The analyses are presented for different geographic locations over Saudi Arabia such as deserts and mountains. These geographic locations have varying degrees to which the atmosphere and surface are coupled together. At the surface, the radiative energy is coupled to the atmosphere for all surfaces, because the composition and temperature profile of the atmosphere determine the incoming fluxes at the surface. At the top of the atmosphere (TOA), the upwelling radiation may be decoupled from the surface fluxes due to the intervening atmosphere. The desert, with no vegetation, may at first appear a simple geographic region for developing energy budget scheme. The atmosphere is coupled to the surface through strong sensible heat fluxes, which can result in mixed-layer depths of 5 km in summer. Therefore, a coupling between the surface and TOA fluxes is expected. On the other hand, advection of atmospheric water vapor and dust storms tends to decouple the energy budget at the top of the atmosphere from the surface physical properties (Ackerman and Inoue, 1994).

Maps of monthly mean clear sky outgoing longwave radiation and clear sky albedo at the top of the atmosphere for January, April, July, and October 1989 are shown in Fig. 1 and Fig. 2 respectively. These figures reveal many interesting features related to the clear sky circulation patterns such as dry zones and regions of subsidence. Regions of subtropical dry zones over Saudi Arabia are characterized by high albedo and high outgoing long wave radiation and this phenomenon is more pronounced over Empty Quarter desert. The longwave radiation in January and April has low longwave due to the lack of shortwave radiation. This reflects the persistence of subsidence, lack of clouds, and low humidity. Figure 2 shows that the Empty Quarter desert is a highly reflective area whereas reflectivity decreases towards West, East, and Southwest of the Kingdom.

Maps of monthly average regional contour map all sky outgoing longwave radiation and all sky albedo at the top of the atmosphere for January, April, July, and October 1989 are shown in Fig. 3 and Fig. 4 respectively. These figures reveal many interesting features related to the circulation patterns and cloudiness. The major precipitation zones over the Kingdom are characterized by low longwave radiation and high albedo, which results from the presence of cumulus clouds. Figures 3 and 4 show the different areas over the region that have cases of cloud cover (high albedo), and low outgoing longwave radiation.

a. Clear sky albedo of January 1989



b. Clear sky albedo of April 1989

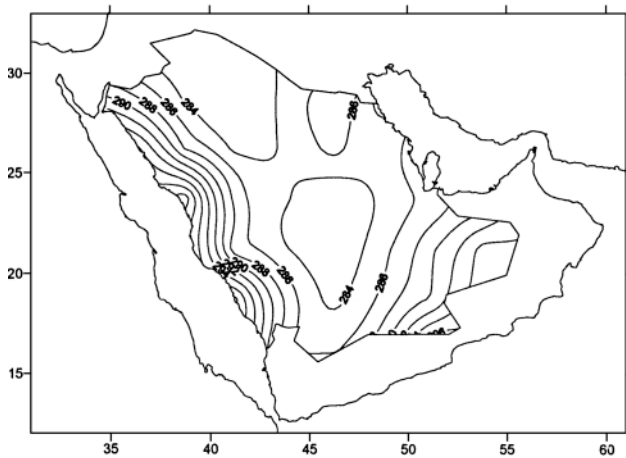
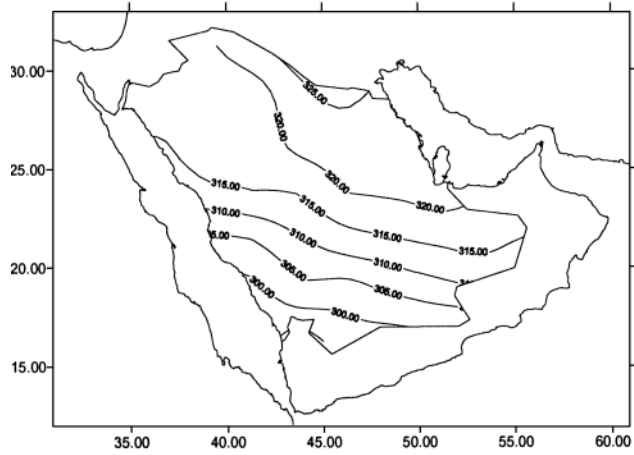


FIG. 1. Clear sky emitted longwave radiation at the top of the atmosphere, ( $Wm^{-2}$ ) for (a) January, (b) April, (c) July and (d) October 1989.

c. Clear sky albedo of January 1989



d. Clear sky albedo of October 1989

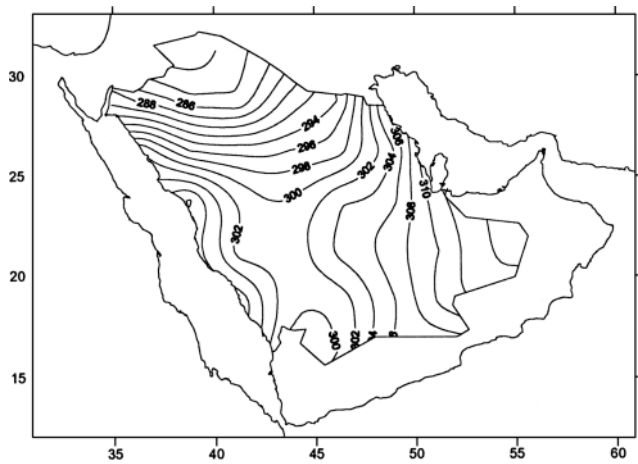
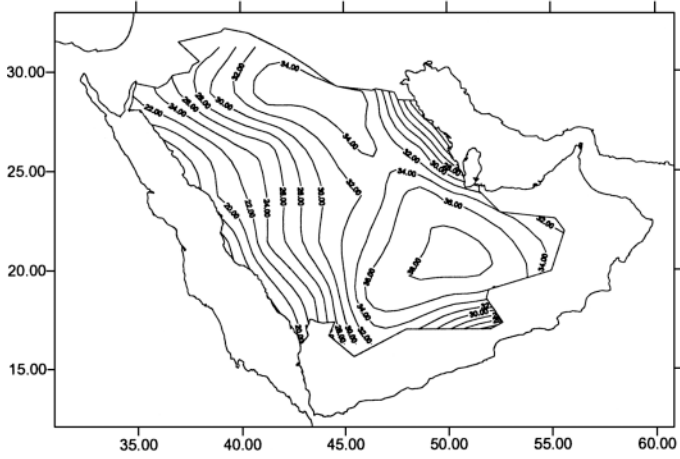


FIG. 1. Contd.

a. Clear sky albedo of January 1989



d. Clear sky albedo of April 1989

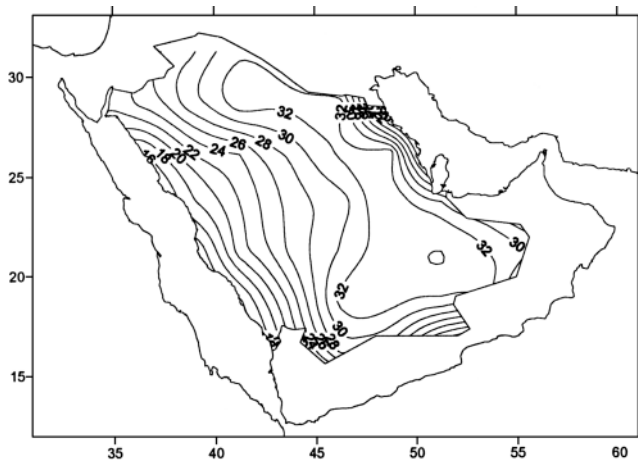
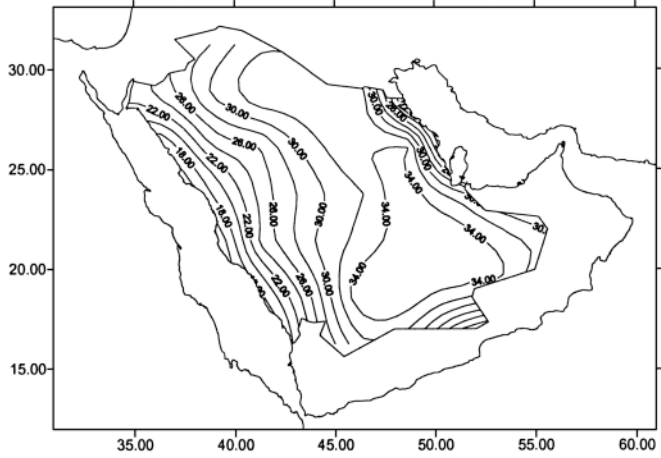


FIG. 2. Clear sky planetary albedo (%) for (a) January, (b) April, (c) July and (d) October 1989.

c. Clear sky albedo of July 1989



d. Clear sky albedo of October 1989

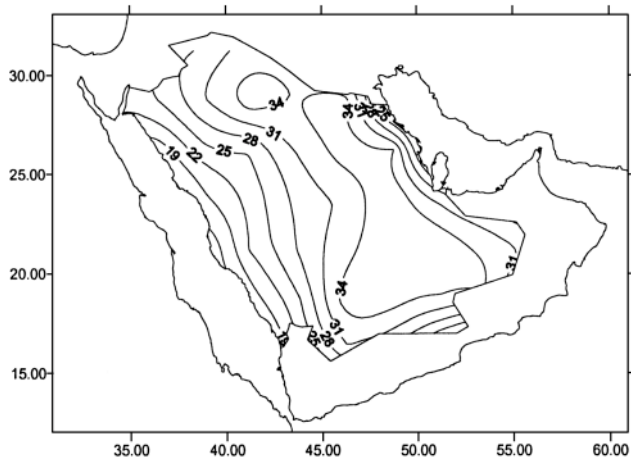


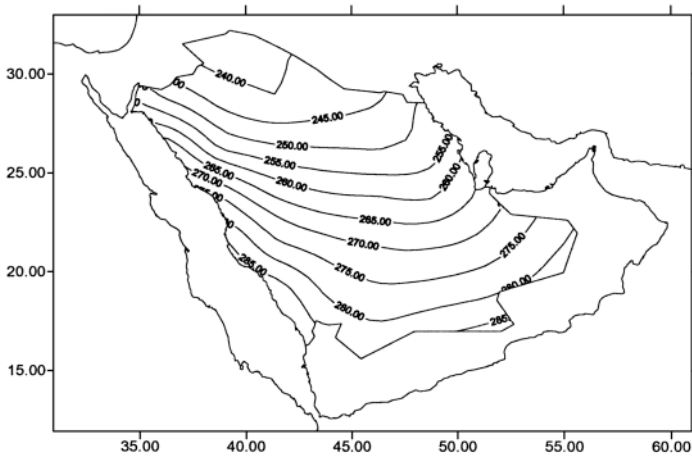
FIG. 2. Contd.



However, some areas of the region are generally clear or scattered clouds most of the time during the selected months which minimizes the difference between all sky and clear sky cases such as Empty Quarter region which has large value of albedo due to the high reflectivity of the surface.

The comparison between clear sky and all sky cases for each month indicates that all sky longwave is less than clear sky longwave, and all sky albedo is larger than clear sky albedo except the desert areas over Empty Quarter which has

a. All sky longwave of January 1989



b. All sky longwave of April 1989

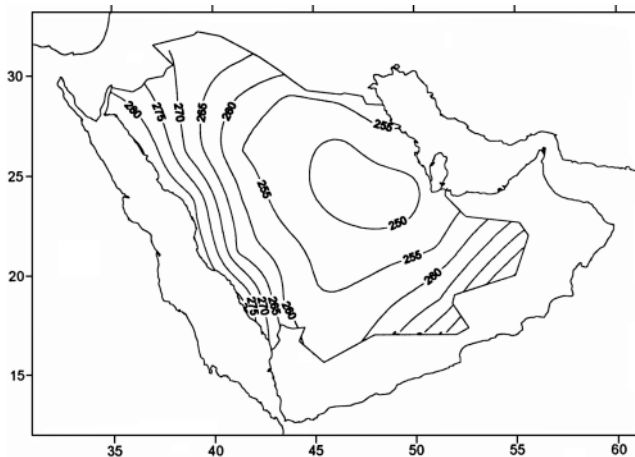
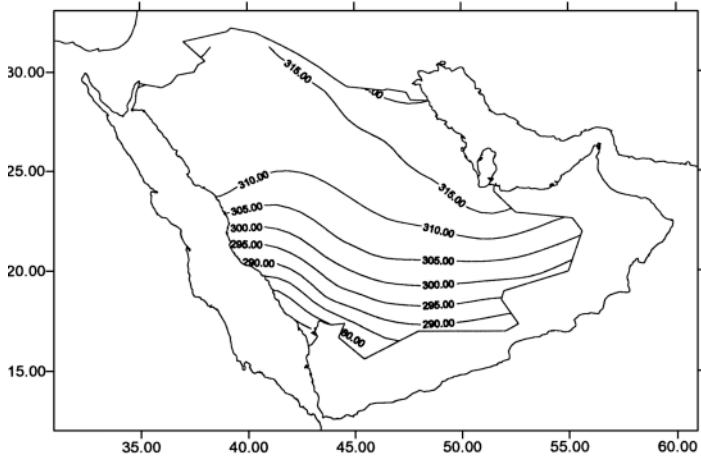


FIG. 3. All sky emitted longwave radiation at the top of the atmosphere, ( $\text{Wm}^{-2}$ ) for (a) January, (b) April, (c) July and (d) October 1989.

c. All sky longwave of July 1989



d. All sky longwave of October 1989

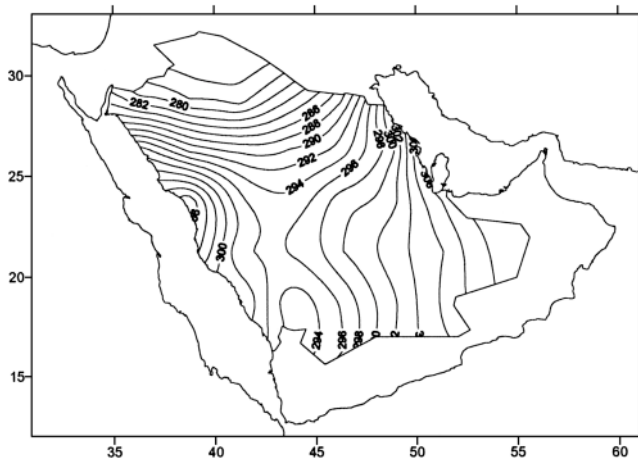
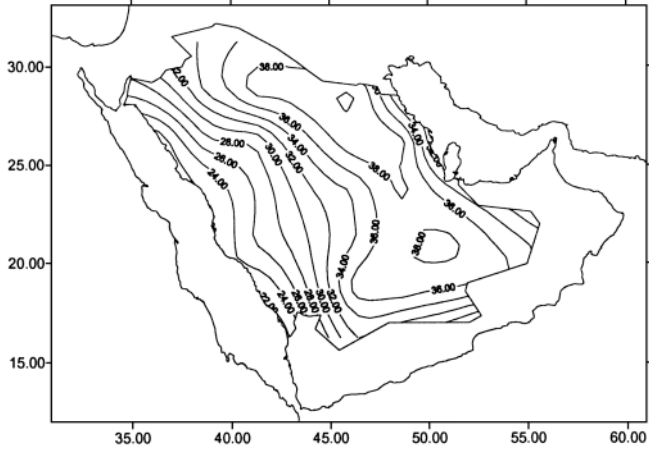


FIG. 3. Contd.

a. All sky albedo of January 1989



d. All sky albedo of April 1989

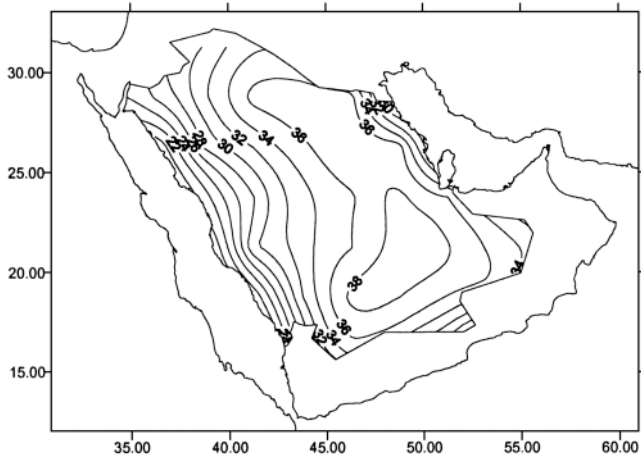
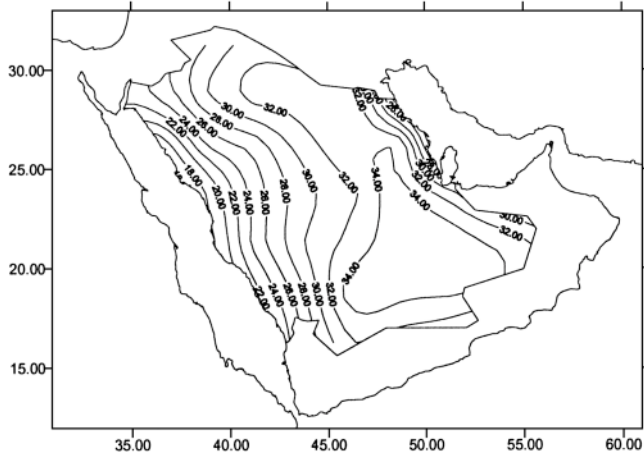


FIG. 4. All sky planetary albedo (%) for (a) January, (b) April, (c) July and (d) October 1989.

c. All sky albedo of July 1989



d. All sky albedo of October 1989

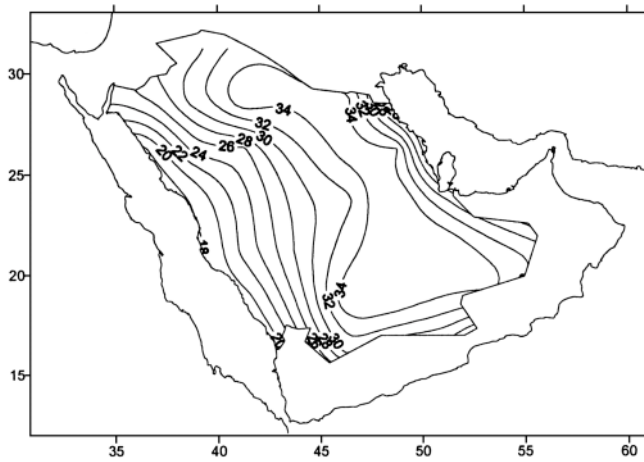


FIG. 4. Contd.

no clouds during the whole month. For example, a map for January 1989 clear sky longwave shown in Fig. 1 looks very much like the January 1989 all sky map shown in Fig. 3 in that the features of both maps are very similar in the general structure of contours and the location of high and low values of longwave. However, there are significant differences especially over desert regions. The subtropical dry zones over Empty Quarter desert, central areas, southeast, and most of Saudi Arabia are characterized by high outgoing longwave radiation with high albedo during the month of July for both all sky and clear sky conditions. The southwest of the country is characterized by low outgoing longwave radiation with low albedo during the same month for both all sky and clear sky conditions.

All results show seasonal shift of longwave and albedo with different months. The seasonal shifting of these features is apparent through months as shown in Fig. 1 and 3 for longwave radiation and Fig. 2 and 4 for albedo. The seasonal patterns of albedo and long wavelength Earth radiation are complex due to the properties of the Earth's surface and atmospheric properties. Monthly mean of outgoing longwave radiation and albedo show that all sky conditions emits less amounts of longwave radiation than clear sky. On the other hand mean of all sky albedo is larger than clear sky cases (Table 1). Table 1 shows the standard deviation of the longwave radiation and albedo with respect to local zonal mean longwave radiation and albedo for all latitudes over Saudi Arabia. The longwave mean ranges from  $257.1 \text{ Wm}^{-2}$  to  $307.7 \text{ Wm}^{-2}$  over the region. Highest value is observed at July clear sky whereas the minimum value in January all sky cases (Table 1). The longwave standard deviation ranges from  $10.6 \text{ Wm}^{-2}$  to  $27.9 \text{ Wm}^{-2}$  over the region. Highest value is found at January all sky cases whereas the minimum value in April clear sky cases. The albedo mean ranges from 20.9% to 30.6 % over the region. Highest value is observed at January all sky whereas the minimum value in April clear sky cases (Table 1). The albedo standard deviation ranges from 5.5% to 8.7% over the region. Highest value is found at January all sky cases whereas the minimum value in July all sky cases.

**TABLE 1. Mean and standard deviation (S.D.) for longwave radiation and albedo for both clear sky and all sky cases for January, April, July, and October, 1989.**

	Month							
	January		April		July		October	
	Mean	S.D.	Mean	S.D.	Mean	S.D.	Mean	S.D.
All sky (lw) $\text{Wm}^{-2}$	257.1	27.9	267.2	21.6	293.7	22.1	284.9	20.4
Clear sky (lw) $\text{Wm}^{-2}$	272.1	21.6	289.2	10.6	307.7	13.6	294.5	13.3
All sky (albedo) (%)	30.6	8.7	26.6	7	24.5	5.5	25.2	6.6
Clear sky (albedo) (%)	23.3	8.1	20.9	7.1	22.1	6.8	22.1	7.1

#### 4. Longwave Cloud Forcing Over Saudi Arabia

At any instant more than half of the earth is cloud-covered. Cloudiness is a fundamental variable for the Earth's radiative balance. Clouds also may respond to climate change in such a way as to modulate climate sensitivity significantly. Clouds have two competing effects on Earth's energy balance; through the reflection of incoming solar radiation and the trapping of the longwave radiation, leading to cloud greenhouse effect. For understanding the role of clouds in the climate system, cloud radiative forcing is a useful indicative. Changes in cloud forcing can result from changes in cloud amount or cloud type, atmospheric conditions, or surface properties. In order to understand how clouds affect the Earth's radiation budget, cloud-forcing is calculated as the difference between the clear sky fields and the total fields (Harrison, *et al.*, 1990). Cloud-forcing comes from the idea that the climate system is ultimately driven by energy from the sun. Anything that changes the amount or distribution of energy absorbed or emitted by the Earth will affect climate and so can be considered a climate forcing. The radiative characteristics of clouds are expressed in terms of cloud radiative forcing defined as the difference between the observed cloudy sky radiation and the clear sky radiation at the top of the atmosphere for the longwave (LW) as follows:

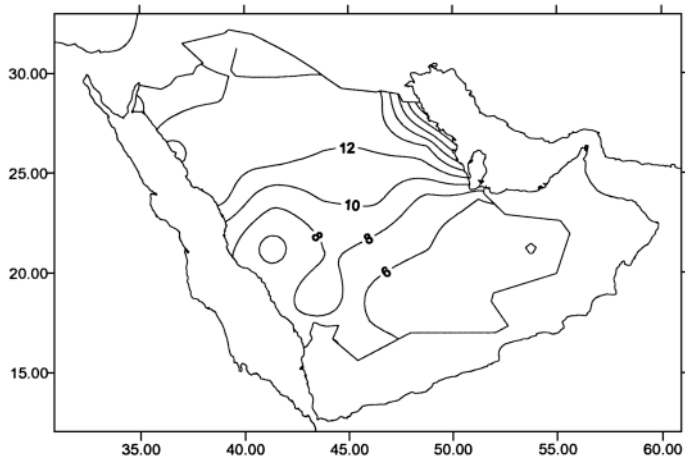
$$\text{LWCF}_{\text{top}} = \text{LW}_{\text{clear sky}} - \text{LW}_{\text{all sky}} \quad (1)$$

Where  $\text{LWCF}_{\text{top}}$  is the longwave cloud forcing at the top of the atmosphere, the  $\text{LWCF}_{\text{top}}$  demonstrates the amount by which clouds reduce the outgoing longwave radiation at the top of the atmosphere. Positive values mean less longwave cooling of the planet.

To try to gain an understanding of how clouds affect Earth's atmosphere system, outgoing longwave radiation change in the presence of clouds will be examined. Figure 5 shows how much cloud affect the amount of radiation emitted into space by comparing data from the same locations during cloudy and non-cloudy days. The difference between different areas in the region comes from the different types of clouds and different times of the year. In April, the cloud reduces longwave radiation at the top of the atmosphere over the whole area. In the Southwest areas above the Asir Mountains during months of July, cumulonimbus clouds reach deep into the top of the troposphere and their tops are cold. Other areas at different months have stratocumulus clouds which are shallow and their tops are warm. Cloud-free areas in the subtropics emit the largest amounts of longwave radiation and this will minimize the difference between all sky and clear sky cases as shown in Fig. 5. Cloud's behavior depends on complex dynamic and thermodynamic couplings between the surface and atmosphere. Table 2 shows the longwave cloud forcing for January, April, July,

and October 1989. The cloud forcing at the top of the atmosphere equals  $15 \text{ Wm}^{-2}$  for January,  $22 \text{ Wm}^{-2}$  for April,  $14 \text{ Wm}^{-2}$  for July, and  $10 \text{ Wm}^{-2}$  for October 1989. Thus, compared to a cloud free atmosphere, the January mean cloudiness, as it was present, reduces the outgoing longwave radiation for the total earth-atmosphere system by about 6%, for the month of April by about 8%, for the month of July by about 5%, and for the month of October by about 3%.

a. Cloud forcing long wave for January 1989



b. Cloud forcing long wave for April 1989

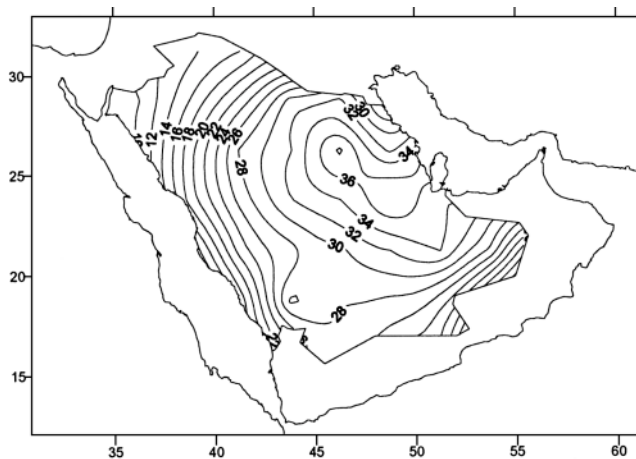
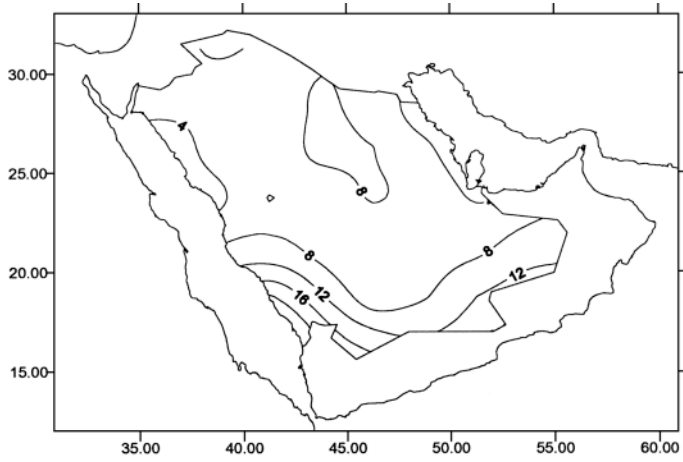


FIG. 5. Averaged long wave cloud forcing at the top of the atmosphere ( $\text{LWCF}_{\text{top}} \text{ Wm}^{-2}$ ) for (a) January, (b) April, (c) July and (d) October 1989.

c. Cloud forcing long wave for July 1989



d. Cloud forcing long wave for October 1989

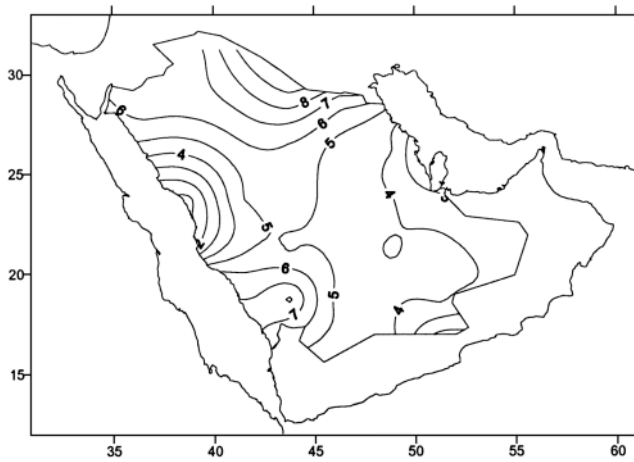


FIG. 5. Contd.



**TABLE 2. Longwave mean of radiation budget for both clear sky and all sky and cloud forcing at the top of the atmosphere (TOA) for January, April, July, and October, 1989.**

	Month			
	January	April	July	October
All sky (lw) $\text{Wm}^{-2}$	257.1	267.2	293.7	284.9
Clear sky (lw) ( $\text{Wm}^{-2}$ )	272.1	289.2	307.7	294.5
Cloud forcing (lw) $\text{Wm}^{-2}$	15	22	14	10
Cloud forcing / clear sky (%)	5.51	7.6	4.55	3.26

### 5. Linear Correlation Between Albedo and Longwave Radiation

In the previous section, the geographical distributions of the monthly mean of albedo, longwave radiation, and cloud forcing were discussed. It was assumed that the temporal variability in albedo and longwave radiation results primarily from variations in cloudiness and the incoming solar radiation. Therefore the resulting patterns of variability appear to be consistent with this interpretation.

In this section, the relationship between local changes in albedo and longwave radiation will be examined. Scatter diagrams of albedo versus longwave radiation for 9 locations are shown in Fig. 6. Solid lines in each of the 10 panels represent a linear fit to the monthly mean values for the whole year. The data points have a negative slope which is well represented by the line of regression. Scatter about the line of regression may be caused by fluctuations in the type of cloud, and the temperature or humidity in the field of view. Hartmann and Short (1980) showed that the slope of the line is a sensitive indicator to cloud regimes, and is also controlled by cloud amounts over the area.

For clear sky desert conditions, the ERBE-measured longwave flux is more sensitive to the state of the atmosphere than the albedo. A relationship can be expected between albedo and longwave radiation, such that as the surface gets darker, the albedo gets lower, with longwave radiation increasing due to an increased surface temperature. Ackerman and Inoue (1994) found little correlation ( $r = 0.15$ ) between the ERBE measured albedo and outgoing longwave radiation. Their analyses indicated that the top of the atmosphere (TOA) fluxes and surface properties are decoupled spectrally. In the present study, a similar correlation ( $r = 0.38$ ) was found between the ERBE measured albedo and outgoing longwave radiation at some locations over the Kingdom. These locations were selected for different parts of the Kingdom as shown in Table 3. The relationship between the surface albedo and clear sky longwave at top of the atmosphere are affected by the variability of Earth's surface background. The spectral decoupling may result from different spectral characteristics of the at-

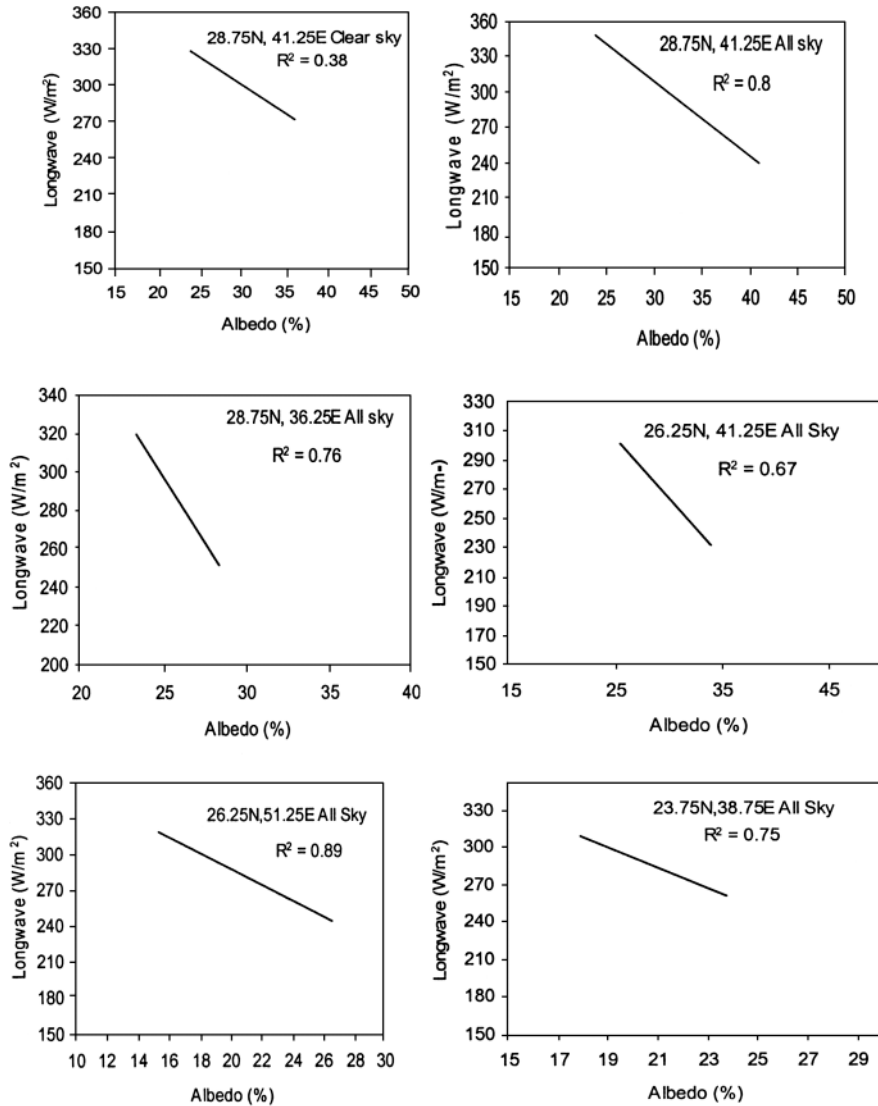


FIG. 6. Scatter diagrams of outgoing longwave radiation versus albedo for various geographical locations over the region of Saudi Arabia. The line represents a least squares fit to the monthly data points for the whole year of 1989.

mosphere, which are more transparent to the shortwave (SW) than the longwave (LW). In addition to atmospheric variability, surface characteristics also play an important role in determining TOA fluxes. For example, different soil types with the same albedo may have different specific heats, for the same amount of absorbed solar energy. As result, one soil may raise its temperature faster than another which results in decoupling the SW properties from LW radiation. Smith (1986) have demonstrated that the mean properties of the desert surface are controlled by radiative exchanges at the surface.

The coupling of all sky albedo and all sky outgoing longwave radiation results in strong relationship ( $R^2 = 0.80$ ) at the same location (Fig. 6). For this region, when the albedo increases, the LW flux at the top of the atmosphere correspondingly decreases. This strong relationship is due to the smooth properties of clouds compared with earth surface. The outgoing longwave radiation is controlled by cloud top temperature. Table 3 summarizes the relationship results for the selected locations over the region.

**TABLE 3. A summary of  $R^2$  values for different locations over the region of study.**

Latitude	Longitude	Sky condition	$R^2$
28.75	41.25	clear sky	0.38
28.75	41.25	all sky	0.80
28.75	36.25	all sky	0.77
26.25	41.25	all sky	0.67
26.25	51.25	all sky	0.89
23.75	38.75	all sky	0.75
23.75	46.25	all sky	0.77
18.75	43.75	all sky	0.73
16.25	43.75	all sky	0.86

## 6. Summary and Conclusions

Monthly average outgoing longwave radiation and monthly average albedo have been addressed to investigate how changing surface and cloud conditions affect the energy budget at the top of the atmosphere. The linear square relations between outgoing longwave radiation and albedo have been presented. Geographical variations of Earth's albedo, and Earth radiation (long wavelength radiation) received by satellites from cloud free areas and cloudy areas of the Earth's surface were explored. The patterns observed were controlled by the variations in seasonal radiation received from the sun and varying properties of

the Earth's surface. These comparisons between cloud free and cloudy areas, will give a clear idea of reflectivity caused by clouds and that caused by Earth surface properties such as deserts and high lands. Also, these data sets show what areas of the region clouds persistently cover, and what areas are generally cloud free. The subsidence zone is sometimes associated with low clouds which increases longwave radiation and decreases albedo, while the precipitation zones associated with tall clouds reduce the longwave radiation and increase albedo. The desert regions are characterized by an absence of clouds and low humidity.

The longwave mean ranged from  $257.1 \text{ Wm}^{-2}$  to  $307.7 \text{ Wm}^{-2}$  over the region. Highest value was in July clear sky whereas the minimum value was in January all sky cases. The longwave standard deviation ranged from  $10.6 \text{ Wm}^{-2}$  to  $27.9 \text{ Wm}^{-2}$  over the region. Highest value was in January all sky cases whereas the minimum value was in April clear sky cases. The albedo means ranged from 20.9% to 30.6% over the region. Highest value was in January all sky whereas the minimum value was in April clear sky cases. The albedo standard deviation ranged from 5.5% to 8.7% over the region. Highest value was in January all sky cases whereas the minimum value was in July all sky cases.

Radiative forcing of clouds is dependent on the temperature of the source of the radiation from this cloud. If the tops of clouds are the source of the radiation, and if the temperature of the cloud top decreases with increasing height, it can be expected that there will be less thermal radiation from a high cloud than from a low cloud, because the top of the high cloud is colder than the top of the low cloud. The cloud forcing at the top of the atmosphere equaled  $15 \text{ Wm}^{-2}$  for January,  $22 \text{ Wm}^{-2}$  for April,  $14 \text{ Wm}^{-2}$  for July, and  $10 \text{ Wm}^{-2}$  for October 1989. Thus compared to a cloud free atmosphere, the January mean cloudiness, as it was present, reduced the outgoing longwave radiation for the total earth-atmosphere system by about 6%, for the month of April by about 8%, July by about 5%, and October by about 3%. The largest reduction percentages due to cloudiness were during the month of April and the smallest reduction was during October.

The relationship between local changes in albedo and longwave radiation was discussed. The data points had a negative slope which was well represented by the line of regression. Scatter about the line of regression might be caused by fluctuations in the type of cloud, and the temperature or humidity in the field of view. For clear sky desert conditions, the ERBE-measured longwave flux was more sensitive to the state of the atmosphere than the albedo. A weak correlation ( $r = 0.38$ ) between the ERBE measured albedo and outgoing longwave radiation was found at some locations over the Kingdom. The relationship between the surface albedo and clear sky longwave at top of the atmosphere was

affected by Earth's surface variability. The coupling of all sky albedo and all sky outgoing longwave radiation resulted in strong relationship ( $r = 0.80$ ) at some location. For this region, when the albedo increased, the LW flux at the top of the atmosphere correspondingly decreased. This strong relationship was due to the smooth properties of clouds compared with Earth's surface.

### References

- Ackerman, S.A. and Inoue, T.** (1994) Radiation energy budget studies using collocated AVHRR and ERBE observations, *J. Appl. Meteor.*, **33**: 370-378.
- Barkstrom, B. R., Harrison, E., Smith, G., Green, R., Kibler, J., Cess, R. and ERBE Science Team** (1989) Earth Radiation Budget Experiment (ERBE) archived and April 1985 results, *Bull. Amer. Meteor. Soc.*, **70**: 1254-1262.
- Bess, T.D. and Smith, G.L.** (1993) Earth Radiation Budget: Results of outgoing longwave radiation from Nimbus-7, NOAA-9, and ERBS Satellites, *J. Appl. Meteor.*, **32**: 813-824.
- Harrison, E.F., Minnis, P., Barkstrom, B.R., Ramanathan, V., Cess, R.D. and Gibson, G.G.** (1990) Seasonal variation of cloud radiative forcing derived from the Earth Radiation Budget Experiment, *J. Geophys. Res.*, **95**: 18687-18703.
- Hartmann, D.L. and Short D.A.** (1980) On the use of Earth Radiation Budget Statistics for studies of clouds and climate, *J. Atmos. Sci.*, **37**: 1233-1250.
- Jacobowitz, H., Smith W.L., Howell H.B., Nagle F.W. and Hickey, J.R.** (1979) The first 18 months of planetary radiation budget measurements from the Nimbus 6 ERB experiment, *J. Atmos. Sci.*, **36**: 501-507.
- Manabe, S. and Wetherald, R.T.** (1967) Thermal equilibrium of the atmosphere with a given distribution of relative humidity, *J. Atmos. Sci.*, **24**: 241-259.
- Smith, E.A.** (1986) The structure of the Arabian heat flow. Part 1: Surface energy budget, *Mon. Wea. Rev.*, **114**: 1068-1083.
- Smith, W.L., Hickey J., Howell H.B., Jacobowitz H., Hilleary D.T. and Drummond A.J.** (1977) Nimbus 6 Earth Radiation Budget Experiment, *Appl. Opt.*, **16**: 306-318.

## نتائج الأشعة ذات الموجات الطويلة المنبعثة ونسبة الانعكاسية فوق المملكة العربية السعودية من بيانات تجربة ميزانية الإشعاع الأرضي

عبدالرحمن خلف الخلف

قسم الأرصاد، كلية الأرصاد والبيئة وزراعة المناطق الجافة،  
جامعة الملك عبد العزيز، جدة - المملكة العربية السعودية

المستخلص. اعتبرت التغيرات في نسبة الانعكاسية والأشعة ذات الموجات الطويلة المنبعثة في أعلى الغلاف الجوي، والمستخرجة من بيانات تجربة ميزانية الإشعاع الأرضي، كدالة متغيرة تعتمد على خصائص الغلاف الجوي، أو عندما تحتوي السماء على السحب، كما تعتمد أيضا على خصائص سطح الأرض، أو عندما تكون السماء خالية من السحب.

كما استخدمت أيضا بيانات الأشعة ذات الموجات الطويلة المنبعثة والانعكاسية، لدراسة العلاقة بين التغير في كمية السحب، والظواهر الإقليمية للدورة العامة للغلاف الجوي، مثل مواطن الهطول، وأماكن تجمع السحب، إضافة إلى أماكن هبوط الهواء إلى أسفل الغلاف الجوي. تتطلب هذه الطريقة قياسات بيانات الأشعة ذات الموجات الطويلة المنبعثة، والانعكاسية لتقييم نسبة أهمية هذين العنصرين للدورة العامة للغلاف الجوي. كما أن طريقة الدراسة اعتمدت التغير الزمني والمكاني لهذه البيانات لمعرفة الميزانية الإشعاعية لمختلف المناطق الجغرافية، مثل الصحاري، والجبال، والمناطق الساحلية. تشير النتائج إلى وجود علاقة واضحة بين التغير في الأشعة ذات الموجات الطويلة المنبعثة، والانعكاسية مع الظواهر العامة للغلاف الجوي، والتي ترتبط بتغير كمية السحب، كما تمت دراسة تأثير التغير الجغرافي على تكون السحب وربطها بالدورة العامة للغلاف الجوي، مثل مواقع الهطول وأماكن وجود السحب بشكل مستمر، ومناطق هبوط الهواء من طبقات الجو العليا. تتراوح متوسطات قيم الأشعة ذات الموجات الطويلة بين ٢٥٧ وات/م<sup>٢</sup> و ٣٠٧ وات/م<sup>٢</sup>، كما تتراوح قيم الانحراف المعياري بين ٦, ١٠ وات/م<sup>٢</sup> و ٩, ٢٧ وات/م<sup>٢</sup>،

أما بالنسبة لقيم المتوسطات للانعكاسية فهي بين ٩, ٢٠٪ و ٦, ٣٠٪ كما أن الانحراف المعياري للانعكاسية يتراوح بين ٥, ٥٪ و ٧, ٨٪ فوق المنطقة. تشير النتائج إلى أن القوة الإشعاعية ذات الموجات الطويلة في أعلى الغلاف الجوي تساوي ١٥ وات/م<sup>٢</sup> لشهر يناير، و ٢٢ وات/م<sup>٢</sup> لشهر إبريل، و ١٤ وات/م<sup>٢</sup> لشهر يوليو، وتساوي ١٠ وات/م<sup>٢</sup> لشهر أكتوبر. وبالمقارنة مع الغلاف الجوي الخالي من السحب، تؤدي السحب - كما هي موجودة - في شهر يناير إلى نقصان كمية الأشعة الخارجة من سطح الأرض ومن الغلاف الجوي بنسبة ٦٪، وبنسبة ٨٪ لشهر إبريل، ٥٪ لشهر يوليو، وأخيرا بنسبة ٣٪ لشهر أكتوبر. تمت دراسة علاقة الارتباط بين كمية الإشعاع المنبعث من السماء الخالية من السحب، ونسبة الانعكاسية فوق بعض أجواء المملكة، فتبين أن العلاقة بينهما ضعيفة (معامل التقدير  $R^2 = 0,38$ )، بينما تكون هذه العلاقة قوية بين السماء الغائمة، أو عندما تحتوي السماء على السحب، ونسبة الانعكاسية الكلية (انعكاسية سطح الأرض مضافا إليها انعكاسية الغلاف الجوي) علاقة قوية، حيث تساوي في بعض الأماكن (معامل التقدير  $R^2 = 0,80$ ).